Studies in Engineering and Exact Sciences
ISSN: 2764-0981

Image segmentation of Capsicum annuum chili with lighting problems using the otsu method

Segmentação de imagens de chili Capsicum annuum com problemas de iluminação usando o método de otsu

DOI: 10.54021/sesv3n4-001

Recebimento dos originais: 10/09/2022
Aceitação para publicação: 11/10/2022

Osbaldo Vite Chávez
PhD in Engineering
Institución: Universidad Autónoma de Zacatecas
Dirección: Posgrado en Ingeniería y Tecnología Aplicada, UAIE, 98000, Zacatecas, México
Correo electrónico: osvichz@uaz.edu.mx

Jorge Flores–Troncoso
PhD in Engineering
Institución: Centro Regional de Desarrollo Espacial en el Estado de Zacatecas (CREDEZ)
Dirección: Complejo Quantum, 98000, Zacatecas, México
Correo electrónico: jflorest@uaz.edu.mx

Jorge Ulises Muñoz Minjares
PhD in Engineering
Institución: Universidad Autónoma de Zacatecas
Dirección: Campus Jalpa, 99601, Jalpa, Zacatecas, México
Correo electrónico: ju.munoz@uaz.edu.mx

Roberto Olivera Reyna
Master's Degree in Engineering
Institución: Universidad Autónoma de Zacatecas
Dirección: Campus Jalpa, 99601, Jalpa, Zacatecas, México.
Correo electrónico: roliverar@uaz.edu.mx

Eduardo García Sánchez
PhD in Engineering
Institución: Universidad Autónoma de Zacatecas
Dirección: Campus Siglo XXI, 98000, Zacatecas, México
Correo electrónico: eduardog@uaz.edu.mx

Reynel Olivera Reyna
Master's Degree in Engineering
Institución: Universidad Autónoma de Zacatecas
Dirección: Campus Jalpa, 99601, Jalpa, Zacatecas, México
Correo electrónico: reynel@uaz.edu.mx

RESUMO
A iluminação não uniforme captada numa imagem devido à luz natural ou iluminação mal condicionada pode causar uma segmentação deficiente dos objectos numa imagem quando se utilizam técnicas tradicionais de limiar. Este artigo apresenta resultados experimentais melhorados utilizando o método de Otsu na segmentação de imagens do chile capsicum annuum (conhecido no México como chile caribe ou chile güero) com problemas de claridade e sombras geradas pela luz natural. Os testes experimentais são realizados no pressuposto de que as imagens cinzentas com maior contraste mostram uma melhoria significativa na segmentação. Os resultados obtidos são apresentados de forma comparativa com as diferenças percentuais de melhoria utilizando a métrica de Dice e Jaccard.

Palavras-chave: segmentação, imagens, iluminação, capsicum annuum, método de otsu.

RESUMEN
La iluminación no uniforme captada en una imagen, debida a la luz natural o a una iluminación mal acondicionada, puede provocar una mala segmentación de los objetos de una imagen cuando se utilizan las técnicas tradicionales de umbralización. Este trabajo presenta resultados experimentales mejorados utilizando el método de Otsu en la segmentación de imágenes de chile capsicum annuum (conocido en México como chile caribe o chile güero) con problemas de brillo y sombras generados por la luz natural. Las pruebas experimentales se realizan partiendo de la base de que las imágenes grises con mayor contraste presentan una mejora significativa en la segmentación. Los resultados obtenidos se presentan de forma comparativa con las diferencias porcentuales de mejora utilizando las métricas Dice y Jaccard.

Palabras clave: segmentación, imágenes, iluminación, capsicum annuum, método otsu.

1 INTRODUCTION

The science development has innovated technologies for the benefit of humanity, addressing the problems presented in different sectors such as agriculture, commercial, industrial, educational, and health, among others (Cantú, 2019). In the marketing of agricultural products, the visual aspect is very important to evaluate their quality based on different physical properties such as color,

shape, and size. A manual visual inspection generates high operating costs and time-consuming. This activity is susceptible to human error, thus inducing difficulties to standardize the selection results (Vite et. al. 2022). The inaccuracies that occur in the selection of an agricultural product affect its commercial value. So, the detection, classification, and recognition of fruits and vegetables as a subfield of object recognition have introduced important challenges (Vite et al. 2022, Belan et al. 2020, Yuan et al. 2015).

In artificial vision, image segmentation is a very important step to analyze and interpret the acquired image in various applications such as medical, agriculture, robotic vision, material science, geographic imaging, etc. (Sha et al., 2016, Goh et al., 2018, Lu et. al., 2017, Munoz-Minjares et al., 2021). One of the principal problems in artificial vision systems is the images acquisition in an uncontrolled lighting environment. This phenomenon generates images with low contrast, saturated areas, brightness, and shadow problems. Thus, they also can hide information also hide information and make it difficult for any inspection algorithm to provide an adequate selection of product quality. A dim lighting can cause a low signal-to-noise ratio, resulting in an noisy image. Furthermore, non-uniform lighting can significantly hinder the segmentation process by using basic thresholding techniques such as Otsu's (Yuan et al., González et al., 2002, Ng et al. 2006).

Threshold techniques are important for various applications due to their simplicity and efficiency. They are commonly used to separate objects from the background of the image in product quality inspection tasks (Sha et al., 2016, Liu et al., 2015, Lu et al., 2017). The basic idea of a thresholding method is to automatically obtain an optimal gray level threshold value t to separate the object of interest from the background. The value of a threshold t is obtained based on the gray level distribution in the histogram of a digital image (Goh et al., 2018, Lei et al., 2019). There are two kind of thresholds, local and global. The local threshold is based on gray intensity level of the histogram to choose several threshold levels. The value of the local threshold depends on local statistics, such as range, variance, among other adjustment parameters, in the pixel neighborhood of the image. The methods that compute a local threshold are tolerant to illumination changes, these are sensitive to noise and thus degrading the image segmentation.

In addition, local threshold methods use more computational processing resources, which generates a great disadvantage against other algorithms. Among the most sophisticated techniques using local thresholds are mentioned in scientific literatura, the Niblack, Gatos, Sauvola, and Bradley algorithms (Bataineh et al. 2017, Cheremkhin et al., 2019, Singh et al., 2012).

Global thresholds are simpler and easier to implement than local thresholds since they select a single value from the histogram of the image, however their result are based on good lighting, i.e. uniform (Yuan et al., 2015, Ng et al., 2006). In a study of global thresholding techniques, Sahoo (Sahoo et al., 1988) was concluded that the Otsu method is one of the best threshold selection methods to discuss. This method selects a threshold value that maximize the variations between classes in the histogram. However, it is only optimal for thresholding a histogram with a bimodal or multimodal distribution, whose distributions are clearly defined in shape and size (Munoz-Minjares et al., 2021). Therefore, the Otsu method is inaccurated if the histogram presents a unimodal or quasi-unimodal distribution (Vite et. al. 2022, Lei et al., 2019, Liu et al., 2015).

The objective of this work is to demonstrate that the object segmentation of capsicum annuum chili images can be improved, despite their problems of brigthness and shadows due to natural light or uncontrolled lighting of the environment. his issue is established assuming that a RGB channel presents a higher contrast to improve the binary segmentation. For this purpose, three experimental tests were carried out using images of the chili species capsicum annuum ("Caribbean chili" or "chile güero" in Mexico) with lighting problems and the Otsu method to perform the segmentation. The results are presented in a comparative form using the Dice and Jaccard metrics to show the quality of the binary segmentation for each test performed. Finally, the percentage improvement differences are obtained.

2 MATERIALS AND METHODS

It was necessary to capture some images using a Logitech HD C270 fixed webcam and 720p/30c/s. The images were captured in an environment with natural lighting environment by using an expanded polystyrene booth located at a horizontal distance of $45\ cm$ between the webcam and the object. This structure is

illustrated in Fig. 1. The size of the booth is $50cm \times 80cm \times 50cm$, which corresponds to the length, width, and height, respectively.

Figure 1. Cabin diagram for image acquisition

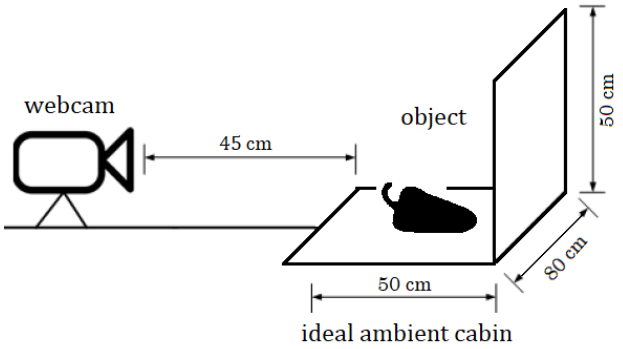

Fig. 2 shows the captured images of the Capsicum annuum pepper. For the experimental tests, only three images were selected, these images presented presented lighting problems with an original size of 1536×2048 pixels ($\boldsymbol{I}_{\mathrm{O}}$). Later, two croppeds of the region of interest, focused on the object, were obtained from each original $\boldsymbol{I}_{\mathrm{O}}$ image. In the cutouts of the images, the background of the object was reduced as shown in Fig. 2. The first group of cropped images was $\boldsymbol{ROI}_1$ with a size of 7.5% pixels (27% $\boldsymbol{I}_{\mathrm{O}}$), and the second group of cropped images was $\boldsymbol{ROI}_2$ with a size of 361×651 pixels (7.5% of $\boldsymbol{I}_{\mathrm{O}}$). Experimental tests of the original and cropped test images were performed by using MATLAB $R2018b$ software. Likewise, it was used a computer with an Intel(R) Xeon(R) CPU E3 1226 v3 @ $3.30\mathrm{GHz}$ processor, and equipped with $8\mathrm{G}$ of RAM. For experimental development, it was proposed one test for each group $\boldsymbol{I}_{\mathrm{O}}$, $\boldsymbol{ROI}_1$, and $\boldsymbol{ROI}_2$, which correspond to the rows of Fig. 2. These tests were performed based on the BWS algorithm (see Algorithm 1), where two grayscale images $\boldsymbol{I}_{g1}$ and $\boldsymbol{I}_{g2}$ were obtained from the selected RGB images.

Figure 2. RGB images used for the tests carried out. Original images $\boldsymbol{I}_{\mathrm{O}}$, cropped images $\boldsymbol{ROI}_1$ and $\boldsymbol{ROI}_2$.

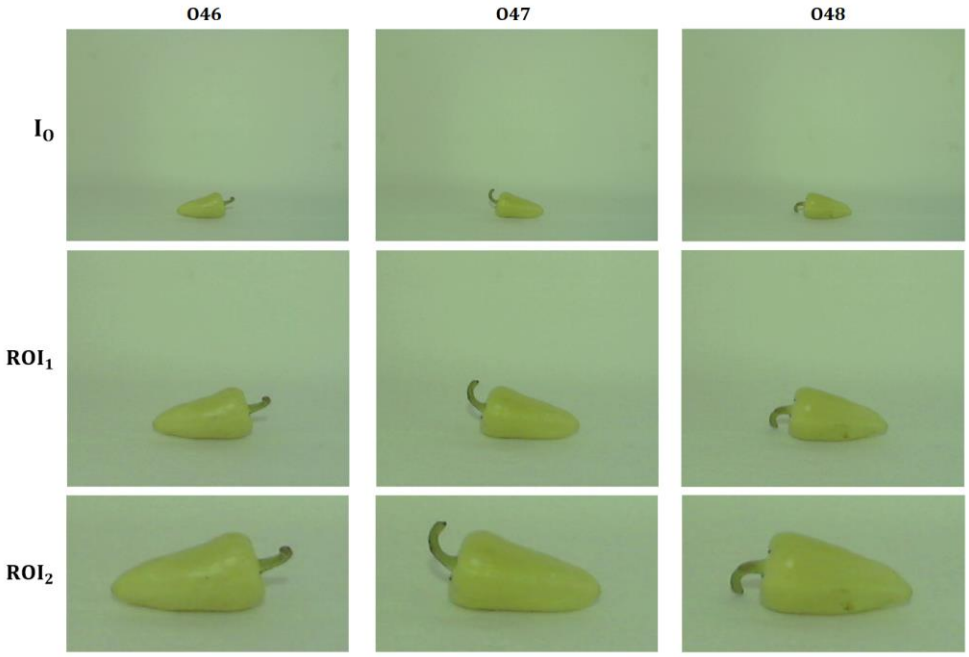

Algorithm 1: Algorithm BWS

$// \ \boldsymbol{I}_{RGB} \leftarrow [\boldsymbol{I}_1, \boldsymbol{I}_2, \ldots \boldsymbol{I}_n \,];$
$// \ \boldsymbol{I}_{b1(n)}, \ \boldsymbol{I}_{b2(n)}, \ \boldsymbol{I}_{b3(n)}, \ \boldsymbol{I}_{b4(n)} \leftarrow binarized \ images;$
$Input: \boldsymbol{I}_{RGB}$
$Output: \boldsymbol{I}_{b1} : \boldsymbol{I}_{b4}$
$1: \boldsymbol{I}_{g1(n)} = [0.29 * R + 0.58 * G + 0.11 * B] \leftarrow \boldsymbol{I}_{RGB}$
$2: [\boldsymbol{I}_R \ \boldsymbol{I}_G \ \boldsymbol{I}_B] \leftarrow \boldsymbol{I}_{RGB}$
$3: \boldsymbol{I}_{g2(n)} = \boldsymbol{I}_B \leftarrow [\boldsymbol{I}_R \ \boldsymbol{I}_G \ \boldsymbol{I}_B] \leftarrow Blue \ Channel \ Selection$
$4: \boldsymbol{h}_g(x) \leftarrow hist[\boldsymbol{I}_{g1}, \boldsymbol{I}_{g2}] \leftarrow Histogram \ operation, \boldsymbol{h}_g(x) \in Z_G^{1x2}$
$5: \boldsymbol{t} \leftarrow \{Graythresh[\boldsymbol{I}_{g1}, \boldsymbol{I}_{g2}], Otsu[\boldsymbol{h}_g(x)]\} \leftarrow Thresholding \ , \boldsymbol{t} \in Z_G^{1x4}$
$6: \boldsymbol{I}_{b1:b4} \leftarrow binarized[(\boldsymbol{I}_{g1}, t_1), (\boldsymbol{I}_{g1}, t_2), \ (\boldsymbol{I}_{g2}, t_3), (\boldsymbol{I}_{g2}, t_4)]$

An image $\boldsymbol{I}_{g1}$ is obtained from the grayscale conversion by using using the Matlab 'rgb2gray' command. This operation is based on the equation 1, which can be applied to each figure of the groups $\boldsymbol{I}_{\mathrm{O}}$, $\boldsymbol{ROI}_1$ and $\boldsymbol{ROI}_2$.

$$\boldsymbol{I}_{g1} = 0.2989 * R + 0.5870 * G + 0.1140 * B \qquad (1)$$

Similarly, the $\boldsymbol{I}_{g2}$ image was obtained by selecting the image of the blue channel of the R, G, and B components of the $\boldsymbol{I}_{\mathrm{O}}$, $\boldsymbol{ROI}_1$ *y* $\boldsymbol{ROI}_2$ images. The blue channel was determined because these images presented greater contrast in gray intensity, which suggests a greater separation between object and background to calculate a better threshold level t and, therefore, a better segmented binary image

(Vite et. al. 2022). In the next step, the histograms of $\boldsymbol{I}_{g1}$ and $\boldsymbol{I}_{g2}$ images are obtained. Consequently, the Otsu method is applied in its two variants 'graythresh'(GTh) and 'otsuthresh'(OTh) of matlab commands. So, thresholds from t_1 to t_4 are obtained respectively to finally obtain the black and white images $\boldsymbol{I}_{b1}$, $\boldsymbol{I}_{b2}$, $\boldsymbol{I}_{b3}$, and $\boldsymbol{I}_{b4}$.

3 EXPERIMENTAL RESULTS AND DISCUSSION

In this section, the experimental tests are compared to corroborate the segmentation improvement of the three groups of images $\boldsymbol{I}_{\mathrm{O}}$, $\boldsymbol{ROI}_1$, and $\boldsymbol{ROI}_2$. The original $\boldsymbol{I}_{\mathrm{O}}$ images present a histogram with a quasi-unimodal shape, while the $\boldsymbol{ROI}_1$ images, with a background reduction of 74.5% of the original images, show a histogram with a tendency towards the bimodal shape. The $\boldsymbol{ROI}_2$ images present a well defined bimodal histogram due to 94% background cut. The results shown in Fig. 3 were obtained by applying the BWS algorithm to the $\boldsymbol{I}_{\mathrm{O}}$ images $(046, 047, 048)$. Due to image processing of $\boldsymbol{I}_{g1}$ and $\boldsymbol{I}_{g2}$, four binary images were obtained, $\boldsymbol{I}_{b1}$, $\boldsymbol{I}_{b2}$, $\boldsymbol{I}_{b3}$, and $\boldsymbol{I}_{b4}$, which are the results of the operations GTh_1, OTh_1, GTh_2, and OTh_2, respectively. In the same way, the tests were performed for the groups of images $\boldsymbol{ROI}_1$ and $\boldsymbol{ROI}_2$, which can be seen in Fig. 4 and Fig. 5.

Figure 3. Results obtained by processing $\boldsymbol{I}_{g1}$ (GTh_1, OTh_1) and $\boldsymbol{I}_{g2}$ (GTh_2, OTh_2) using the $\boldsymbol{I}_{\mathrm{O}}$ $(046, 047, 048)$ images and the BWS algorithm.

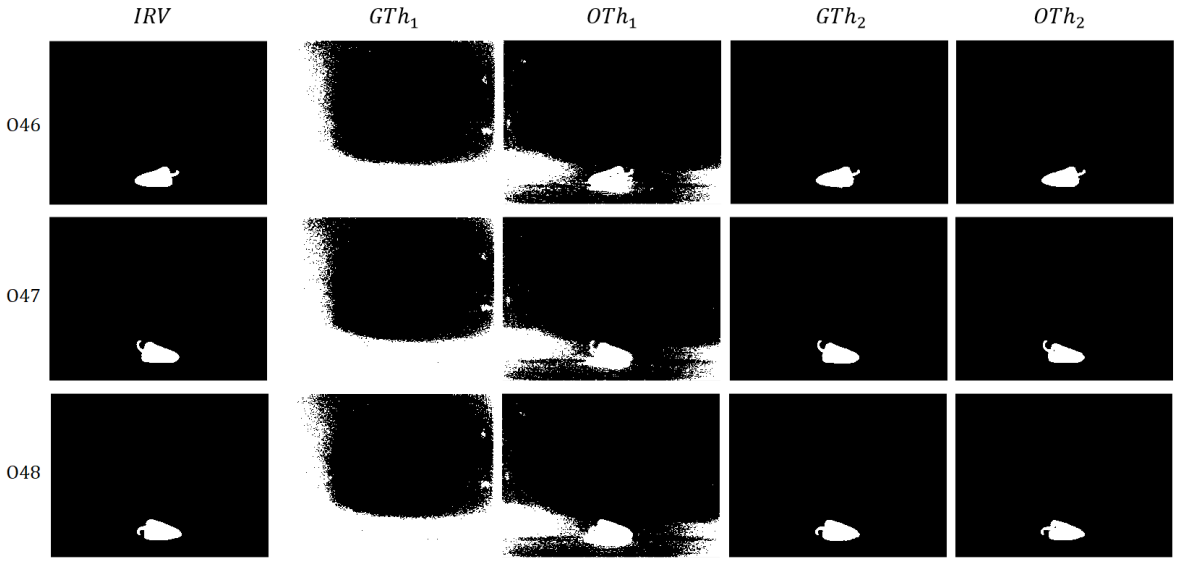

Figure 4. Results obtained by processing $\boldsymbol{I}_{g1}$ (GTh_1, OTh_1) and $\boldsymbol{I}_{g2}$ (GTh_2, OTh_2) using the $\boldsymbol{ROI}_1$ $(046, 047, 048)$ images and the BWS algorithm.

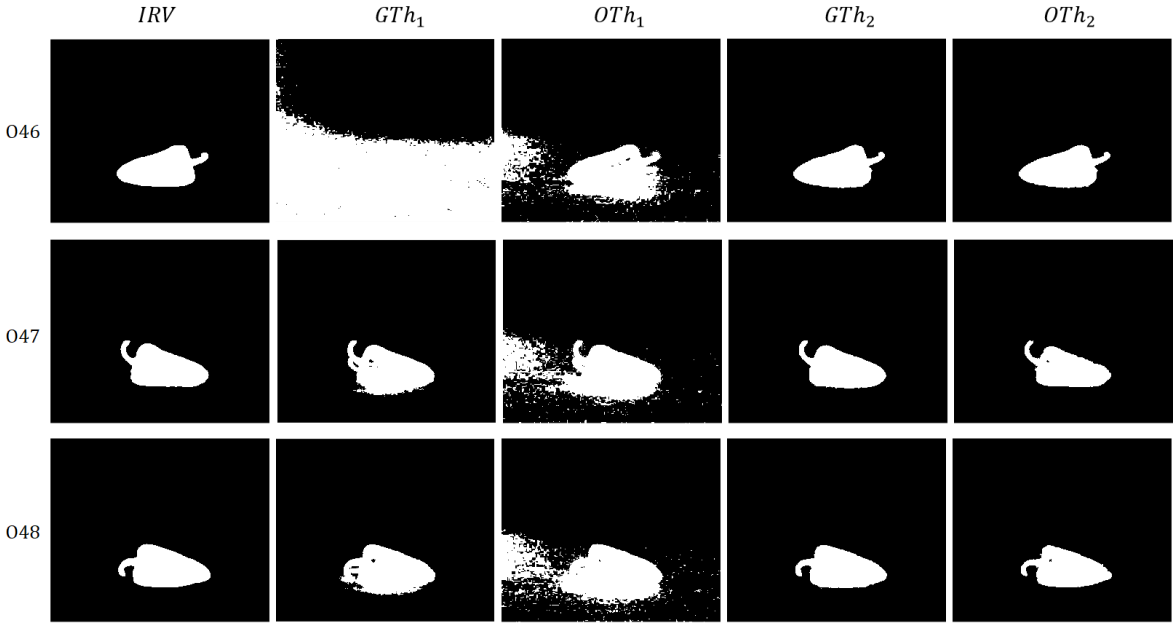

Figure 5. Results obtained by processing $\boldsymbol{I}_{g1}$ (GTh_1, OTh_1) and $\boldsymbol{I}_{g2}$ (GTh_2, OTh_2) using the $\boldsymbol{ROI}_2$ $(046, 047, 048)$ images and the BWS algorithm.

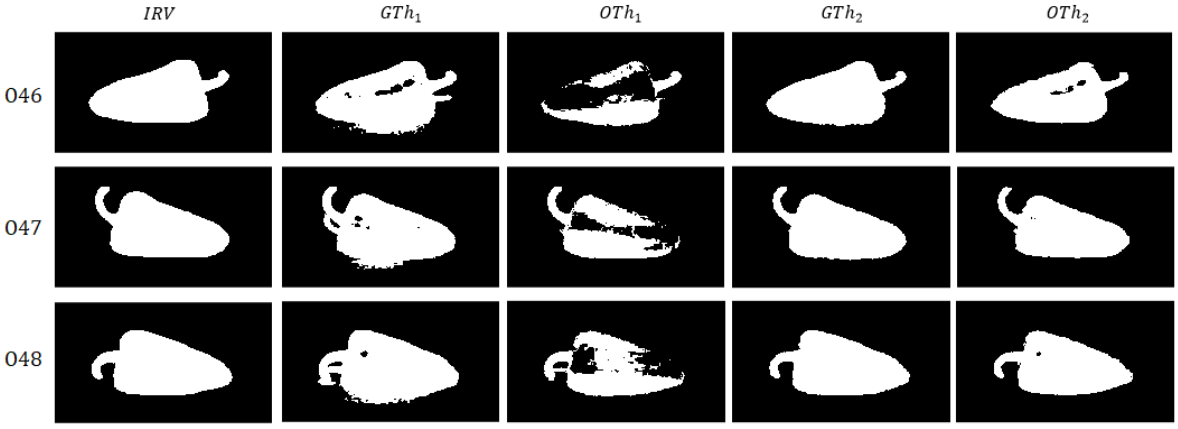

Comparing GTh_1 with GTh_2 and OTh_1 with OTh_2, It can be observed in Fig. 3, Fig. 4 and Fig. 5 that the best results are the GTh_2 and OTh_2 images obtained from the $\boldsymbol{I}_{g2}$ images processed by the BWS algorithm in the three groups of images. Likewise, in the presentation of the results, a ground truth image (IRV) is added in the first position of rows 046, 047 and 048. This image is used for quantitative thresholding comparison. The IRV images were obtained manually and supervised under the criteria of experts in the field. In Fig. 3, comparing each GTh_1 image with IRV, it can be seen that they show very bad background and object segmentation, which represents the worst result. Regarding to the OTh_1 images, they obtained a deficient segmentation with less damage than the GTh_1

images. Contrary, it can be appreciated that the GTh_2 and OTh_2 images show a good segmentation because the object is clearly defined by white pixels and the background by black pixels. The OTh_1 column of $\boldsymbol{ROI}_1$ images were similarly affected in the background and object, resulting in bad segmentation, which can be seen in Fig. 4. The GTh_1 images of rows 047 and 048 show white pixel affectations that do not clearly define the shape of the object, and therefore it is not a good segmentation. In row 046, the GTh_1 image was drastically damaged by white pixels that were not part of the object and that polluted the background, resulting in a deficient segmented image. The cropped images of the rows 046, 047 and 048 of the group $\boldsymbol{ROI}_2$, which are shown in Fig. 5, present problems of gain or loss of white pixels that define the shape of the object. The GTh_1 and OTh_1 image columns show the worst results in this group due to brightness and shadows issues affecting the original captured image. When the GTh_2 and OTh_2 images are compared with the IRV images, it is concluded that they are the best segmentation results of the group. Although a visual comparison of the results shows a noticeable difference, it is required to measure this improvement percentage wise. So, two important metrics, such as Dice and Jaccard, were used to accurately measure the quality of the segmentation. In both measures, values close to $'1'$ represent an efficient segmentation and values close to $'0'$ depict a deficient segmentation.

The results of the Dice and Jaccard metrics in Table 1 correspond to the $\boldsymbol{I}_{\mathrm{O}}$ images in Fig. 3. These results are interpreted by en two comparisons, GTh_1 with respect to GTh_2 and OTh_1 with respect to OTh_2. In the first comparison, the results of the applied metrics reflect the extremes in the segmentation. Here, the values of GTh_2 are greater than 0.9 in all its rows, while GTh_1 does not exceed the value of 0.1. This means that we have excellent segmentation results in GTh_2 and very bad segmentation results in GTh_1. For its part, the second comparison, OTh_2 versus OTh_1, reveals a behavior similar to the previous comparison. The values of the Dice and Jaccard metrics of OTh_2 give values higher than 0.9, while OTh_1 shows values lower than 0.24.

Table 1: Dice and Jaccard metric results for the $\boldsymbol{I}_0$ image group.

Image	Metrics	GTh_1	GTh_2	OTh_1	OTh_2
O46	Dice	0.0719	**0.9530**	0.2294	**0.9550**
	Jaccard	0.0373	**0.9102**	0.1295	**0.9138**
O47	Dice	0.0739	**0.9649**	0.2352	**0.9497**
	Jaccard	0.0384	**0.9322**	0.1333	**0.9042**
O48	Dice	0.0746	**0.9659**	0.2275	**0.9505**
	Jaccard	0.0387	**0.9341**	0.1283	**0.9056**

Table 2 presents the results corresponding to the $\boldsymbol{ROI}_1$ group of images in Fig. 4. Here, the GTh_1 results corresponding to images $O47$ and $O48$ give an average of 0.8, which can be interpreted as a regular segmentation. The Dice and Jaccard values in GTh_1 of image $O46$ are closer to zero and very far from the GTh_2 values, exhibiting a deficient segmentation. On the other hand, the results of the metrics in OTh_1 are 0.5 on average, displaying a bad segmentation. The best results were GTh_2 and OTh_2 with values greater than 0.9, suggesting good segmentation.

Table 2: Dice and Jaccard metric results for the $\boldsymbol{ROI}_1$ image group.

Image	Metrics	GTh_1	GTh_2	OTh_1	OTh_2
O46	Dice	0.2285	**0.9603**	0.6000	**0.9608**
	Jaccard	0.1290	**0.9236**	0.4286	**0.9246**
O47	Dice	0.8952	**0.9648**	0.5928	**0.9492**
	Jaccard	0.8103	**0.9321**	0.4213	**0.9033**
O48	Dice	0.8796	**0.9669**	0.5695	**0.9500**
	Jaccard	0.7851	**0.9360**	0.3981	**0.9048**

Finally, the results of the metrics used in $\boldsymbol{ROI}_2$ are presented in Table 3. The Dice values in GTh_1 represent a regular segmentation that is reflected in Fig. 5. In GTh_2, the Dice and Jaccard values are higher than 0.9. However, the Dice values are closer to one and that suggests good segmentation. Meanwhile, the results in OTh_1 suggest fair to bad segmentation because its results are irregular. The Dice and Jaccard measures in OTh_2 are greater than 0.9 on average, which is interpreted as good segmentation.

Table 3: Dice and Jaccard metric results for the $\boldsymbol{ROI}_2$ image group.

Image	Metrics	GTh_1	GTh_2	OTh_1	OTh_2
O46	Dice	0.8968	**0.9629**	0.6602	**0.9362**
	Jaccard	0.8128	**0.9285**	0.4928	**0.8800**
O47	Dice	0.9201	**0.9644**	0.8040	**0.9504**
	Jaccard	0.8519	**0.9313**	0.6723	**0.9055**
O48	Dice	0.9175	**0.9669**	0.8139	**0.9503**
	Jaccard	0.8475	**0.9359**	0.6862	**0.9053**

In all comparisons of GTh_2 results with GTh_1 and OTh_2 with OTh_1, in all tables, the best results of the metrics were obtained by GTh_2 and OTh_2. This means that, in all comparisons, there is an improvement in the resuls offered by GTh_2 and OTh_2. So, it is corroborated that the images with a higher contrast obtain a better segmentation. Another important aspect to note when we observe this improvement in each table is that it decreases in each test carried out from more to less.

In order to appreciate the improvement obtained by the Dice and Jaccard metrics in each table, the measurement was made by calculating the improvement differences in each of the tables according to the GTh_2 versus GTh_1 and OTh_2 versus OTh_1 comparisons. Later, these differences were multiplied by one hundred, resulting in the Percentage Improvement Difference (PID) obtained by the two comparisons mentioned in each of the results tables. In Fig. 6, the difference in percentage improvement can be seen using the Dice and Jaccard metrics of each of the tables of results obtained from the groups of images $\boldsymbol{I}_{\mathrm{O}}$, $\boldsymbol{ROI}_1$, and $\boldsymbol{ROI}_2$.

Figure 6. Percentage improvement difference results in the three tests performed. Above plots Dice PID and below plots Jaccard PID.

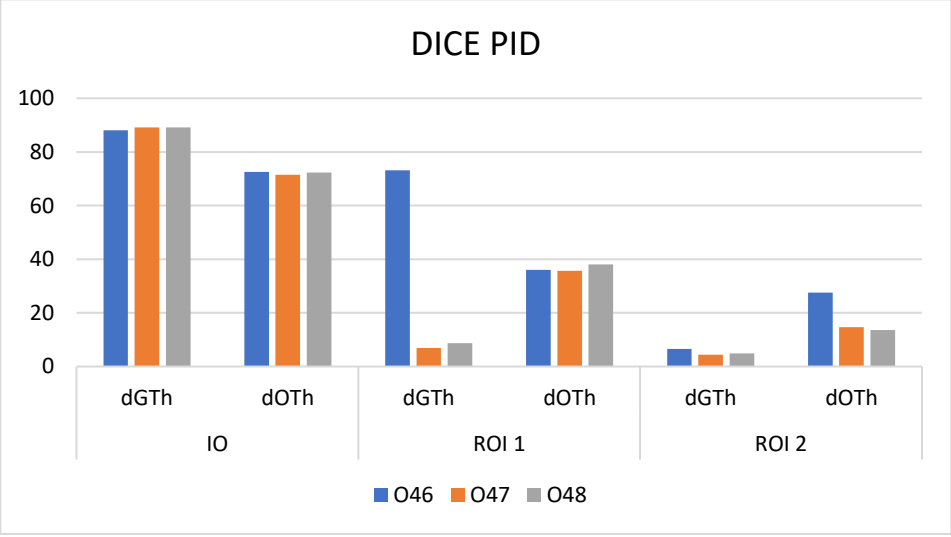

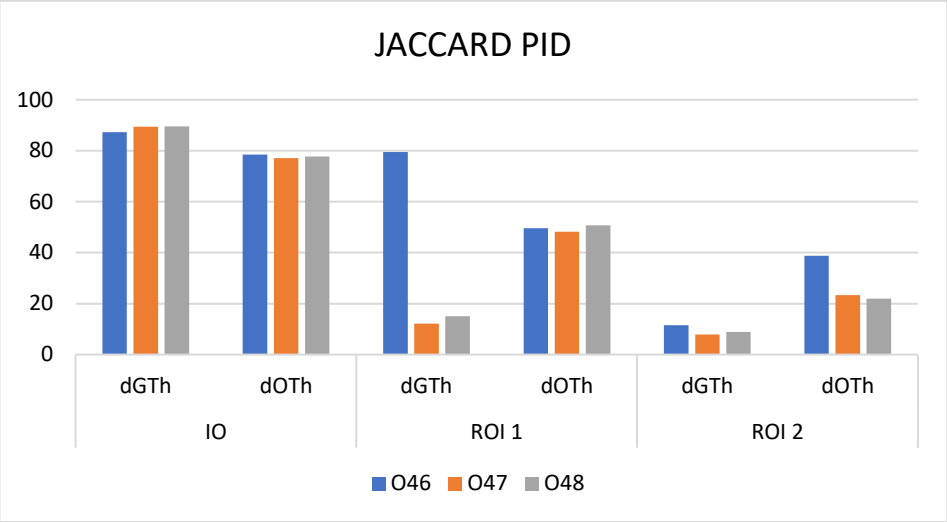

In these graphs, it is also possible to apreciate the decrease in improvement Dice PID and Jaccard PID for each test carried out with the cuts of the images of the groups of $\boldsymbol{ROI}_1$ and $\boldsymbol{ROI}_2$. Looking at Dice PID and Jaccard PID, the smallest PID, in both, appeared in the results where the GTh variant was used.

4 CONCLUSIONS

In the present work, experimental tests were carried out where it was proved that in the grayscale images that present higher contrast, better segmentation results are obtained. This statement is supported by the results obtained with the metrics used. Where, the best results were for GTh_2 and OTh_2 in all their comparisons.

The experimental tests using the Dice and Jaccard metrics resulted in an improvement in all the comparisons of GTh_2 vs GTh_1 and OTh_2 vs OTh_1 in the results tables. Likewise, it was also observed that this improvement decreases with the reduction of the background in each group of $\boldsymbol{ROI}_1$ and $\boldsymbol{ROI}_2$ images. This is corroborated by obtaining the difference in percentage improvement PID in the results of the comparisons made in each group of tables.

These results contribute to decrease the problems of noise in the background and loss of pixels that define the object within the segmentation stage. This step is required to continue towards the classification and recognition of objects from Chile Caribe. Based on these results, it is possible to work with more images of the Caribbean pepper and other agricultural products of interest that present this problem of background non-uniformity, brightness, and shadows.

REFERENCIAS

Cantú-Martínez, P. C. (2019). Ciencia y tecnología para un desarrollo perdurable. *Economía y Sociedad*, *24*(55), 92-112. https://www.scielo.sa.cr/pdf/eys/v24n55/2215-3403-eys-24-55-92.pdf

Vite–Chávez, O., Flores–Troncoso, J., Muñoz–Minjares, J.U., & Rivera–Romero, C.A. (2022). Comparación de resultados en la segmentación de imágenes de chile caribe con problemas de iluminación utilizando el método de Otsu. *Congreso internacional de Investigación e Innovación 2022. Multidisciplinario* (pp 4499-4509). https://www.congresoucec.com.mx/documentos/mem2022/MEMORIA_2022_SEGUNDA_PARTE.pdf

Belan, P. A., de Macedo, R. A. G., Alves, W. A. L., Santana, J. C. C., & Araujo, S. A. (2020). Machine vision system for quality inspection of beans. *The International Journal of Advanced Manufacturing Technology*, *111*(11), 3421-3435. https://link.springer.com/ article/10.1007/s00170-020-06226-5

Yuan, X. C., Wu, L. S., & Peng, Q. (2015). An improved Otsu method using the weighted object variance for defect detection. *Applied surface science*, *349*, 472-484. https://www.sciencedirect.com/science/article/abs/pii/S0169433215011319

Sha, C., Hou, J., & Cui, H. (2016). A robust 2D Otsu's thresholding method in image segmentation. *Journal of Visual Communication and Image Representation*, *41*, 339-351. https://www.sciencedirect.com/science/article/abs/pii/S1047320316302206

Goh, T. Y., Basah, S. N., Yazid, H., Safar, M. J. A., & Saad, F. S. A. (2018). Performance analysis of image thresholding: Otsu technique. *Measurement*, *114*, 298-307. https://www.sciencedirect.com/science/article/abs/pii/S0263224117306243

Lu, Y., & Lu, R. (2017). Histogram-based automatic thresholding for bruise detection of apples by structured-illumination reflectance imaging. *Biosystems Engineering*, *160*, 30-41. https://www.sciencedirect.com/science/article/abs/pii/S153751101730082X

Singh, T. R., Roy, S., Singh, O. I., Sinam, T., & Singh, K. (2012). A new local adaptive thresholding technique in binarization. https://arxiv.org/abs/1201.5227

González, R. C., Woods, R. E., & Masters, B. R. (2009). Digital image processing.

Russ, J. C. (2016). The Image Processing Handbook [Internet].

Ng, H. F. (2006). Automatic thresholding for defect detection. *Pattern recognition letters*, *27*(14), 1644-1649. https://ieeexplore.ieee.org/document/1410499

Liu, L., Yang, N., Lan, J., & Li, J. (2015). Image segmentation based on gray stretch and threshold algorithm. *Optik*, *126*(6), 626-629.

https://www.sciencedirect.com/science/article/ abs/pii/S0030402615000340

Munoz-Minjares, J., Vite-Chávez, O., Flores-Troncoso, J., & Cruz-Duarte, J. M. (2021). Alternative Thresholding Technique for Image Segmentation Based on Cuckoo Search and Generalized Gaussians. *Mathematics*, *9*(18), 2287. https://www.mdpi.com/2227-7390/9/18/2287

Bataineh, B., Abdullah, S. N. H. S., & Omar, K. (2017). Adaptive binarization method for degraded document images based on surface contrast variation. *Pattern Analysis and Applications*, *20*(3), 639-652. https://link.springer.com/article/10.1007/s10044-015-0520-0

Cheremkhin, P. A., & Kurbatova, E. A. (2019). Comparative appraisal of global and local thresholding methods for binarisation of off-axis digital holograms. *Optics and Lasers in Engineering*, *115*,119130. https://www.sciencedirect.com/science/article/abs/pii/S014381 6618313459

Lei, B., & Fan, J. (2019). Image thresholding segmentation method based on minimum square rough entropy. *Applied Soft Computing*, *84*, 105687. https://www.sciencedirect.com/ science/article/abs/pii/S1568494619304685

Sahoo, P. K., Soltani, S. A. K. C., & Wong, A. K. (1988). A survey of thresholding techniques. *Computer vision, graphics, and image processing*, *41*(2), 233-260. https://www.sciencedirect.com/science/article/abs/pii/0734189X88900229